Supporting Information

Low-temperature construction of density Ni single-atom sites on nitrogen-doped carbon to boost dual-channel oxygen reduction

Ke Yang,[a] Sili Liu,[a] Xinhua Li,[a] Wanchuan Jin,[a] Fen Luo,[b] Ruishi Xie,[*a] and Yuanli Li[*a]

[a] Innovation Center of Nuclear Environmental Safety Technology, School of Materials and Chemistry, Analytical and Testing Center, Southwest University of Science and Technology, Mianyang 621010, Sichuan, P. R. China

[b] National Co-
Innovation Center for Nuclear Waste Disposal and Environmental Safety, Southwest University of Sci
ence and Technology, Mianyang, Sichuan, 621010, China

S1. Materials and Instrumentation

Materials and reagents

All chemicals were commercially available and used without further purification. 2,3,6,7,10,11-hexaminotribenzene hexahydrochloride (HATP, 97%) and perfluorinated resin solution (Nafion™, 5%) were purchased from Aladdin Biochemical Technology Co., Ltd. Potassium hydroxide (KOH, 90%), nickel chloride hexahydrate ($NiCl_3 \cdot 6H_2O$, 98%), hydrogen peroxide (H_2O_2, 50%), isopropanol (IPA, 99.7%) and ammonia ($NH_3 \cdot H_2O$, 25%) were purchased from Chengdu Kelong Chemical Co., Ltd. Dimethyl maple (DMSO) was purchased from Chengdu Jinshan Chemical Reagent Co., Ltd. Nitrogen (N_2) and oxygen (O_2) were purchased from Mianyang Changjun Gas Co., Ltd. The ultrapure water (18.25 MΩ·cm) was used in all cases.

Instrumentation

The crystal structure of the products was determined by X-ray diffractometry (PANalytical, Empyrean, Netherlands) with a scan range from 4° to 40°. The morphology of the samples was characterized using a field emission scanning electron microscope (FESEM, Zeiss Ultra 55, Germany) equipped with an energy dispersive spectrometer (EDS) at an accelerating voltage of 10 kV. The high-resolution morphology of the samples was obtained by transmission electron microscopy (TEM, Thermo Fisher Scientific, FEI Tecnai Spirit, America). The distribution of Ni atoms was obtained by JEOL JEM-ARM200F NEOARM atomic resolution transmission electron microscopy (STEM). X-ray photoelectron energy spectrum (XPS) profiles were measured using an X-ray photoelectron spectrometer (Thermo Fisher Scientific, ESCALAB 250Xi, America) under monochromatic Al Kα radiation. The Raman spectra of the samples were recorded on a Renishaw inVia Raman microscope (Renishaw T2AH250V, United Kingdom) with an excitation wavelength of 532 nm. The content of Ni atom in the catalyst was quantitatively determined by the ThermoFIsher-iCAP 6500 inductively coupled plasma atomic emission spectrometer (ICP-OES). The electrochemical data were obtained by the electrochemical workstation (CHI 760E) and the rotating ring disk electrode.

X-ray absorption fine structure (XAFS) spectroscopy was carried out using the *RapidXAFS* 2M (Anhui Absorption Spectroscopy Analysis Instrument Co., Ltd.) by transmission mode at 20 kV and 20 mA, and the Si (551) spherically bent crystal analyzer with a radius of curvature of 500 mm was used. The samples were pelletized as disks of 13 mm diameter with 1 mm thickness using graphite powder as a binder and measured at room temperature.

S2. Preparation of Samples

Preparation of Ni-HITP

First, 20 mg of HATP was ultrasonically dissolved in 20 ml of DMSO solution and stirred at 50 °C for 10 minutes, which was recorded as A solution. 14.205 mg of $NiCl_3 \cdot 6H_2O$ was dissolved in 4 mL of ultrapure water to obtain B solution. Then the B solution was slowly dropped into the A solution and stirred for 5 min. 100 µL of $NH_3 \cdot H_2O$ was added to the A solution. The reaction temperature was increased to 60 °C and remained for 24 h. The product was washed with ethanol and ultrapure water 3 times alternately and dried in a vacuum oven at 60 °C.

Preparation of Ni-O@NC

The preparation of Ni-O@NC is similar to the above method, except that the A solution obtained in the first step is different. Specifically, 20 mg of HATP was ultrasonically dissolved in 20 ml of DMSO solution. Then 2 mL of H_2O_2 was added, and the obtained solution was put into the ice-water bath to react for 30 min to be recorded as A solution.

S3. Electrochemical measurements

The collection efficiency of the ring disk electrode was determined by using a one-electron reversible couple of the ferricyanide system in $K_3[Fe(CN)_6]$ solution. The Pt ring electrode was immersed in N_2-saturated 0.5 M KCl solution containing $K_3[Fe(CN)_6]$ (10 mM). The disk potential (I_d) was scanned between -0.3 and 1 .0 V with a sweep rate of 10 $mV \cdot s^{-1}$. The ring potential (I_r) was set as 1.1 V. The ferricyanide reduced to ferrocyanide at the disk electrode when the voltage of the disk swept to the negative trend. And then the ferrocyanide oxidized back into ferricyanide at the ring electrode.

The collection coefficient (N) is calculated as 0.44 using the following formula.

$$N = -\frac{I_r}{I_d}$$

Electrochemical measurements were performed on the electrochemical workstation equipped with a standard three-electrode electrochemical cell. The electrolyte is a N_2- or O_2-saturated 0.1 M KOH solution. The catalyst ink, a platinum mesh, and a Hg/HgO electrode were used as the work electrode, counter electrode, and reference electrode, respectively. After tens of cyclic voltammetric scans, the linear scanning voltammetric (LSV) curves were measured at a rate of 10 $mV \cdot s^{-1}$. The catalyst ink was made by mixing 5 mg of sample with conductive carbon black (1:1) and dispersing them into 730 μL of ultrapure water, 250 μL of ethanol, and 20 μL of Nafion. After that, 5 μL of homogeneous catalytic ink was loaded onto an RRDE with a diameter of 4 mm, and the catalyst loading was about 0.2 mg·cm^{-2}.

The measured potentials were converted to reversible hydrogen electrode (RHE) using the following equation:

$$E_{(vs.\,RHE)} = E_{(vs.Hg/HgO)} + 0.0592 \times pH + 0.098 \quad (1)$$

The H_2O_2 selectivity (H_2O_2%), Faraday efficiency (FE), and electron transfer number (n) were calculated using the following formulas.

$$H_2O_2\% = 200 \times \frac{I_r/N}{I_r/N + I_d} \times 100\% \quad (2)$$

$$FE = \frac{I_r}{I_d \times N} \times 100\% \quad (3)$$

$$n = 4 \times \frac{I_d}{I_d + I_r/N} \times 100\% \quad (4)$$

S4. Characterization of Samples

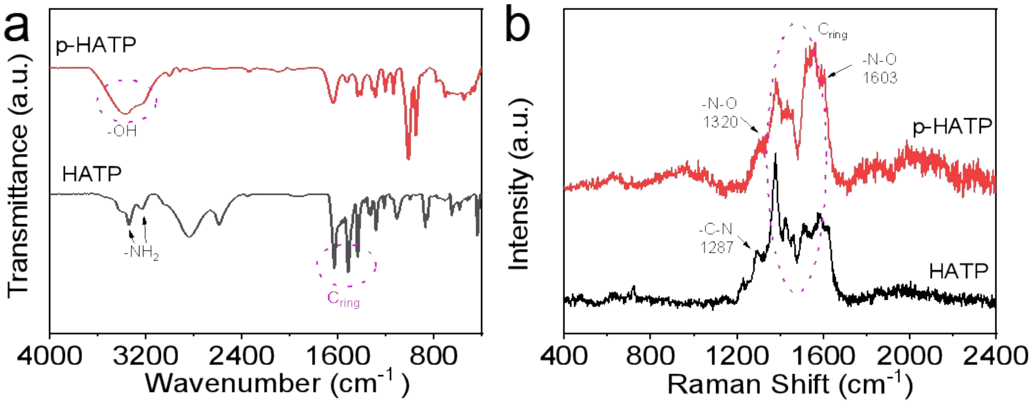

Fig. S1. (a) FTIR spectra and (b) Raman spectra of HATP and p-HATP.

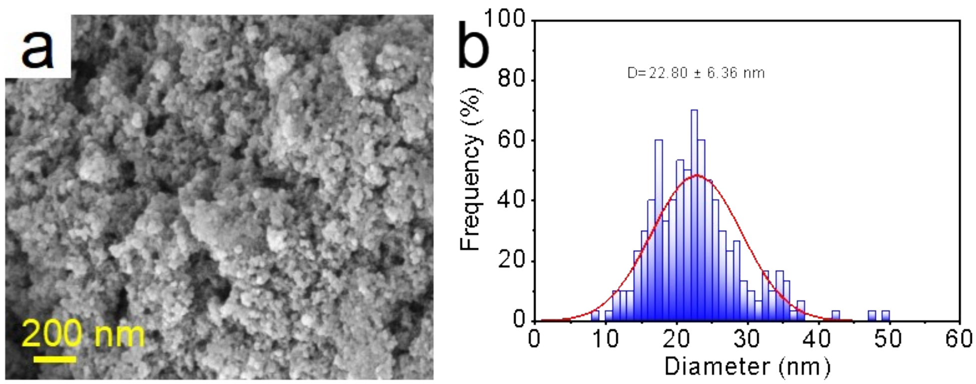

Fig. S2. (a) SEM images of Ni-O@NC. (b) The particle size distribution of Ni-O@NC.

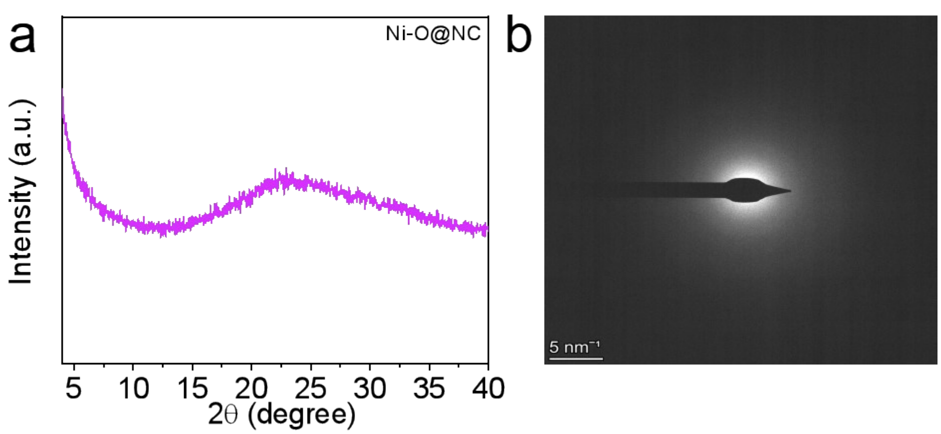

Fig. S3. (a) The XRD pattern and (b) the SAED image of Ni-O@NC.

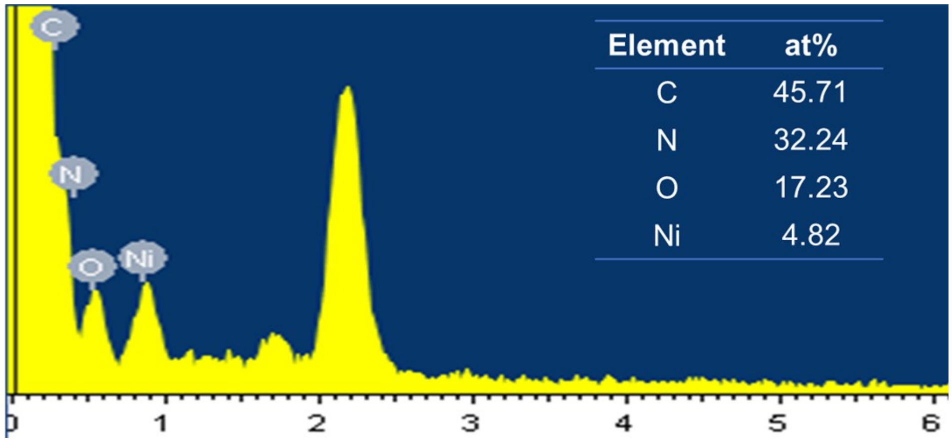

Fig. S4. EDS spectrum of Ni-O@NC.

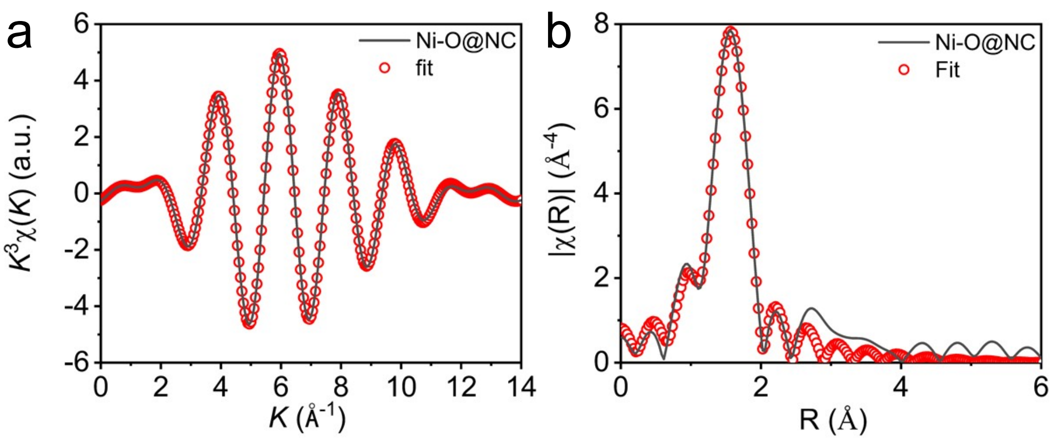

Fig. S5. The EXAFS fitting curves of Ni-O@NC.

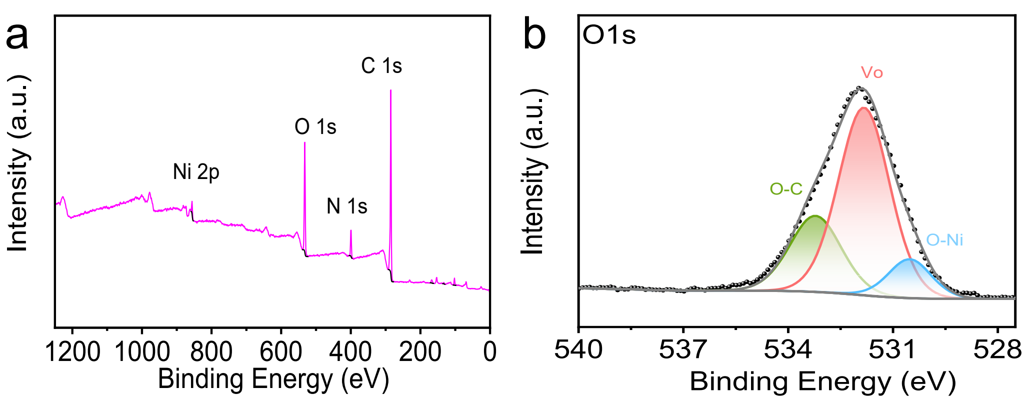

Fig. S6. (a) XPS full spectrum of Ni-O@NC. (b) The high-resolution O 1s XPS spectrum of Ni-O@NC.

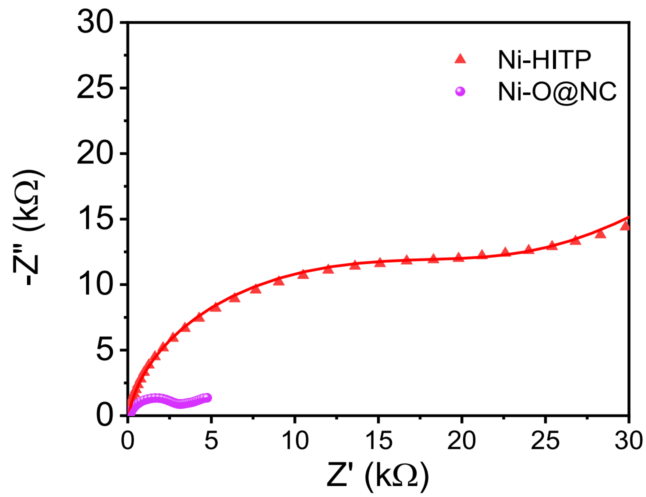

Fig. S7. The Nyquist diagram of Ni-O@NC and Ni-HITP.

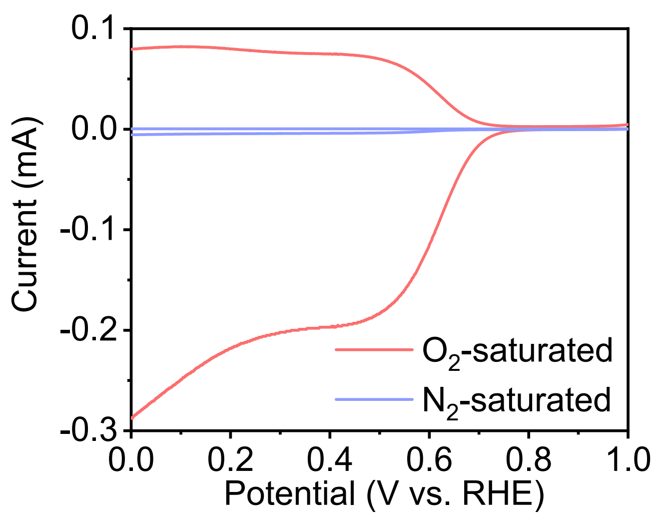

Fig. S8. LSV curves measured in O_2-saturated and N_2-saturated 0.10 M KOH solution.

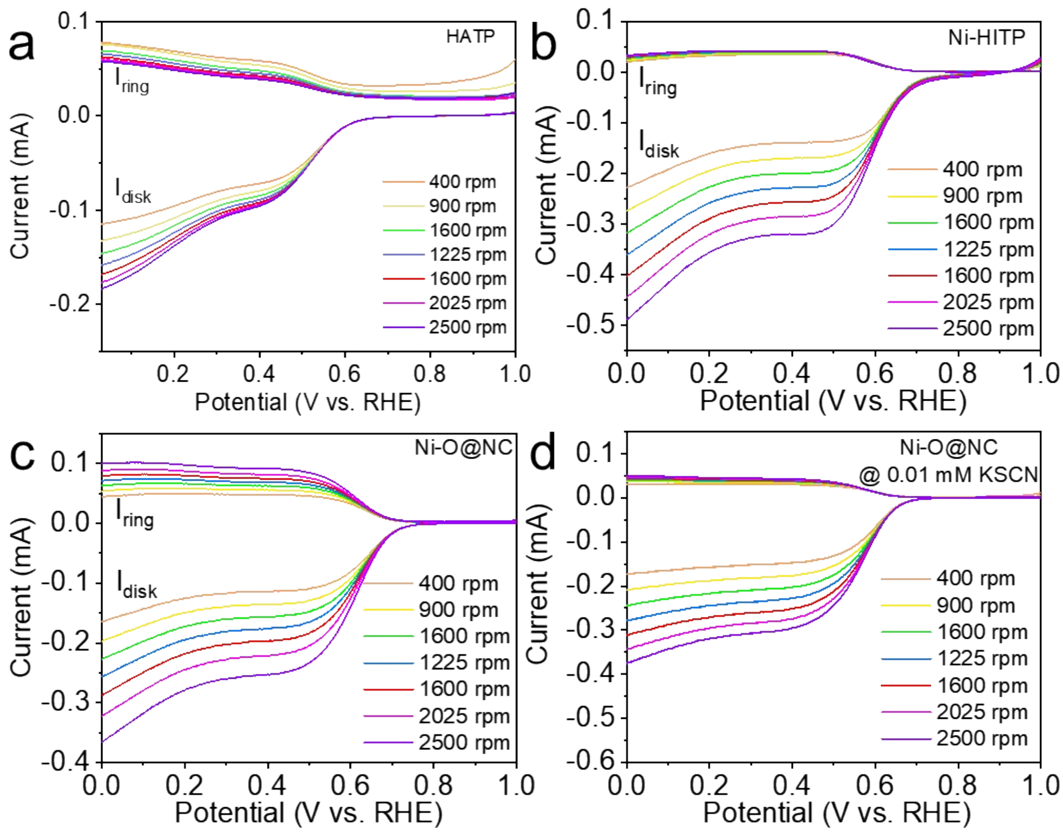

Fig. S9. The LSV curves of (a) HATP, (b) Ni-HITP, and (c) Ni-O@NC measured in O_2-saturated 0.10 M KOH solution. (d) The LSV curves of Ni-O@NC poisoned by 0.01 mM KSCN.

.

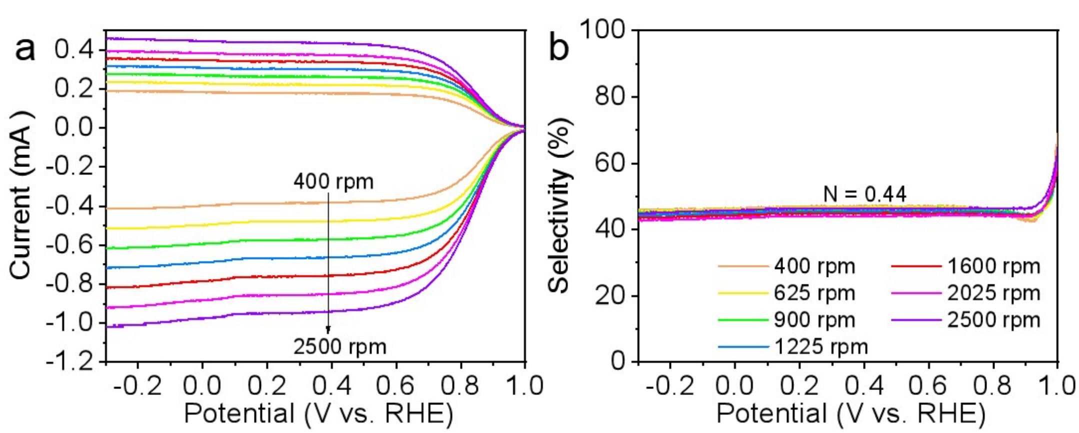

Fig. S10. (a) The LSV curves measured at different rotational speeds in 10 mM $K_3[Fe(CN)_6]$ solution. (b) The experimental collection efficiency determined by the LSV curves in (a).

Table S1. The comparisons between Ni-O@NC and other SACs electrocatalysts.

Catalysts	synthesis condition	temperature	The loading of single atom (wt%)	Ref.
Ni-O@NC	Hydro-thermal synthesis	60 °C	15.9	This work
Fe-N-C	High temperature pyrolysis/H_2 atmosphere	360 °C	8.3	[1]
M-NC SACs (M=Mn、Fe、Ni)	Cascading anchoring	600 °C	12.1	[2]
FeCo-NCH	High-temperature carbonization	800 °C	7.9	[3]
FeSA-CN	Acid etching template method	500 °C	6.3	[4]
Ni-SA/CN	Calcination	500 °C	5.6	[5]
Ni-N-C	Calcination	800 °C	7.8	[6]
COF-Ni(II) complex	Solvothermal method	120 °C	10.6	[7]
Pt SAC	Laser planting method	25 °C	41.8	[8]

Table S2. Structural parameters of Ni-O@NC extracted from the EXAFS fitting. (S_0^2=0.79)

Sample	Path	N	R(Å)	σ^2(Å^2)	ΔE(eV)	R factor
Ni-O@NC	Ni-O	5.4	2.04	0.005	-4.7	0.001

Table S3. The stability of Ni-O@NC and current advanced 2e$^-$ ORR electrocatalysts.

Catalyst	Time	Electron transfer number (n)	H_2O_2 selectivity(%)	Ref.
Ni-O@NC	100 h	~2.1	92.6	This work
$NiSe_2$	12 h	~2.3	90.0	[9]
$ZnSnO_3$	6 h	~2.5	76.0	[10]
CoN_4	90 h	~2.2	94.0	[11]
Ni_{2-x}P-V-Ni	50 h	~2.1	95.0	[12]
ZnO	20 h	~2.2	97.4	[13]
ZnO/N	10 h	~2.3	85.0	[14]
HG-CD-Ph	12 h	~2.1	94.4	[15]
TPDA-BDA	50 h	~2.0	89.7	[16]
Co-N-C	60 h	~2.2	94.0	[17]

Reference

1 S. Yin, Y. Li, J. Yang, J. Liu, S. Yang, X. Cheng, H. Huang, R. Huang, C. T. Wang, Y. Jiang,S. Sun, *Angew. Chem., Int. Ed.* 2024, **63**, e202404766.

2 L. Zhao, Y. Zhang, L. B. Huang, X. Z. Liu, Q. H. Zhang, C. He, Z. Y. Wu, L. J. Zhang, J. Wu, W. Yang, L. Gu, J. S. Hu,L. J. Wan, *Nat. Commun.* 2019, **10**, 1278.

3 Z. Jiang, X. Liu, X.-Z. Liu, S. Huang, Y. Liu, Z.-C. Yao, Y. Zhang, Q.-H. Zhang, L. Gu, L.-R. Zheng, L. Li, J. Zhang, Y. Fan, T. Tang, Z. Zhuang,J.-S. Hu, *Nat. Commun.* 2023, **14**, 1822.

4 Y. Ding, Q. Cheng, J. Wu, T. Yan, Z. Shi, M. Wang, D. Yang, P. Wang, L. Zhang,J. Sun, *Adv. Mater.* 2022, **34**, e2202256.

5 X. Liu, F. He, Y. Lu, S. Wang, C. Zhao, S. Wang, X. Duan, H. Zhang, X. Zhao, H. Sun, J. Zhang,S. Wang, *Chem. Eng. J.* 2023, **453**, 139833.

6 X. Huang, Y. Ma,L. Zhi, *Acta Phys. Chim. Sin.* 2022, **38**, 2011050.

7 H. Zhang, Z. Lin, P. Kidkhunthod,J. Guo, *Angew. Chem., Int. Ed.* 2023, **62**, e202217527.

8 B. Wang, X. Zhu, X. Pei, W. Liu, Y. Leng, X. Yu, C. Wang, L. Hu, Q. Su, C. Wu, Y. Yao, Z. Lin,Z. Zou, *J. Am. Chem. Soc.* 2023, **145**, 13788-13795.

9 Q. Sun, G. Xu, B. Xiong, L. Chen,J. Shi, *Nano Res.* 2023, **16**, 4729-4735.

10 J. Qian, W. Liu, Y. Jiang, Y. Mu, Y. Cai, L. Shi,L. Zeng, *ACS Sustainable Chem. Eng.* 2022, **10**, 14351-14360.

11 S. Chen, T. Luo, X. Li, K. Chen, J. Fu, K. Liu, C. Cai, Q. Wang, H. Li, Y. Chen, C. Ma, L. Zhu, Y.-R. Lu, T.-S. Chan, M. Zhu, E. Cortés,M. Liu, *J. Am. Chem. Soc.* 2022, **144**, 14505-14516.

12 Z. Zhou, Y. Kong, H. Tan, Q. Huang, C. Wang, Z. Pei, H. Wang, Y. Liu, Y. Wang, S. Li, X. Liao, W. Yan,S. Zhao, *Adv. Mater.* 2022, **34**, 2106541.

13 S. Ding, B. Xia, M. Li, F. Lou, C. Cheng, T. Gao, Y. Zhang, K. Yang, L. Jiang, Z. Nie, H. Guan, J. Duan,S. Chen, *Energy Environ. Sci.* 2023, **16**, 3363-3372.

14 P. Xia, T. He, Y. Sun, X. Duan, X. Chen, Z.-S. Zhu, C. Wang, Y. Liu, Q. He,Z. Ye, *ACS Catal.* 2024, **14**, 12917-12927.

15 H. Chen, C. Wang, H. Wu, L. Li, Y. Xing, C. Zhang,X. Long, *Nat. Commun.* 2024, **15**, 9222.

16 J. Liu, W. Zhang, J. Shen, L. Feng, Y. Yao,Q. Peng, *Angew. Chem., Int. Ed.* 2025, **n/a**, e202424720.

17 S. Chen, T. Luo, J. Wang, J. Xiang, X. Li, C. Ma, C.-w. Kao, T.-S. Chan, Y.-N. Liu,M. Liu, *Angew. Chem., Int. Ed.* 2025, **64**, e202418713.